ISBN: 978-3-95450-261-5 ISSN: 2673-7000 doi: 10.18429/JACoW-NAPAC2025-THP030

EMULATION OF TWO-PASS GAIN IN A CAVITY-BASED XFEL VIA SELF-SEEDING AT LCLS

M. D. Balcazar*, A. Lutman, T. Sato, F. J. Decker, Z. Huang, A. Halavanau, D. Zhu
SLAC National Accelerator Laboratory, Menlo Park, CA, USA

Abstract

This work presents an experimental study emulating a two-pass gain scenario in a cavity-based X-ray free-electron laser (CBXFEL) using a self-seeding configuration at LCLS. In this "7+7" arrangement, radiation generated by the first seven hard X-ray undulators (HXUs) is spectrally filtered by a high-resolution self-seeding crystal monochromator and used to seed a second set of seven undulators downstream. This setup mimics the regenerative amplification process expected in the CBXFEL cavity, where the seed pulse is recirculated and overlapped with a second trailing electron bunch. By systematically reducing the number of post-crystal undulators (from 9 to 5), we quantified the spectral amplification ratio by comparing the self-seeded peak signal to the SASE background. These results confirm the feasibility of seeding with the initial seven HXUs and provide a valuable benchmark for extrapolating gain in future two-bunch CBXFEL demonstration experiments.

INTRODUCTION

The cavity-based X-ray free electron laser (CBXFEL) project [1–6] is an ongoing effort at SLAC to develop the next generation of radiation light sources. In contrast to a conventional FEL where the X-ray pulse is generated through a single pass through the undulators, CBXFEL utilizes four Bragg crystal optics to form a *resonant* cavity. Through this process, the cavity output X-rays promise to deliver a fully coherent beam – both transversely and longitudinally – while simultaneously amplifying the pulse via FEL gain.

The CBXFEL project will make use of the first seven hard X-ray undulators (HXUs) at LCLS in combination with the two-bunch operation mode of the electron accelerator to demonstrate two-pass gain. In this scheme, the first electron bunch generates a seed X-ray pulse that is recirculated through the cavity to overlap both temporally and spatially with the second, fresh electron bunch. Seeding is an active area of R&D in the field of FELs, and self-seeding [1] has become a widely adopted technique at facilities worldwide. As this experiment shows, self-seeding techniques can also serve as a stepping stone toward next-generation light sources. In this study, the two-pass gain envisioned by CBXFEL is emulated using a self-seeding approach. Specifically, the seven designated HXUs [7] are used before the self-seeding crystal and another seven after it, a configuration we refer to as "seven plus seven". This emulation aims to demonstrate that the first seven undulators can effectively serve as a seed, and that the subsequent seven can achieve XFEL gain, as promised by the CBXFEL concept.

* mdbm@slac.stanford.edu

EXPERIMENT

Setup

The experiment was conducted using the hard X-ray beamline at LCLS. The output X-ray spectra were measured using the spectrometer located downstream of the XPP hutch in the LCLS X-ray Transport (XRT) tunnel. To emulate the two-pass gain scheme proposed by the CBXFEL project, a hard X-ray self-seeding (HXRSS) setup was utilized. The first seven CBXFEL-designated HXUs were used to generate the initial pulse, followed by additional undulators positioned after the HXRSS crystal as shown in Fig. 1.

The photon energy selected for this study was 7.625 keV and the primary configuration used the (220) reflection in Laue configuration of the HXRSS diamond crystal. At a wavelength of 7.625 keV the crystal Bragg angle is 40.14°, close to the 45° design angle for CBXFEL at 9.831 keV and (400) reflection. The self-seeding setup was then tuned and optimized to achieve its purpose of spectrum filtering and seed creation.

Afterwards, spectral measurements were performed for a sequence of undulator configurations. Starting with 7+13 HXUs and progressively reducing the number of post-crystal undulators to 7+9, 7+8, 7+7, 7+6, 7+5, and finally 7+0 taken as a reference baseline. For each configuration, the resulting X-ray spectrum was recorded using the XRT spectrometer to characterize the evolution of FEL gain.

Experimental Results

The first step in the analysis included a filter on electron beam parameters. The filter was applied to the raw dataset so that only shots within a narrow ~ 2 MeV e-beam energy window were considered [8]. Similarly, shots were filtered based on the beam peak current, keeping those within a 50 A window band centered at the peak of the distribution. This filtering step was crucial for reducing noise and isolating shots with stable beam parameters for meaningful analysis. Following the filter on electron beam parameters, the filtered shots were further screened based on signal strength (maximum intensity) in the detector for each event. Only the top 10% of shots, ranked by peak signal, were kept for the final analysis. This additional filtering step ensured that only the controlled events with strong, well-defined signals contributed to the results.

After filtering, the data was next processed to obtain an average spectrum from the detector. To suppress noise and emphasize spectral features, a Savitzky–Golay filter (window size of 20 and polynomial order 3) was applied to each dataset. This produced a smoothed signal from the detector.

ISBN: 978-3-95450-261-5 ISSN: 2673-7000 doi: 10.18429/JACoW-NAPAC2025-THP030

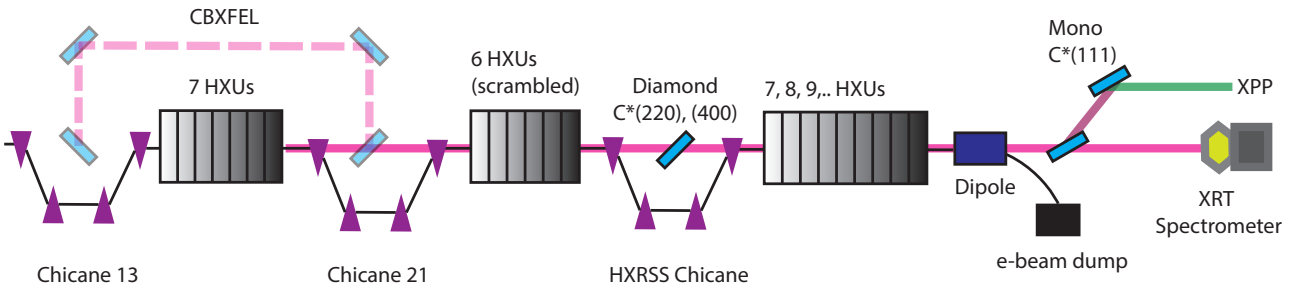

Figure 1: LCLS HXU beamline layout (not to scale) as of 2025: 7 tunable undulator sections are flanked by two electron beam chicanes for CBXFEL experiment, followed by 6 undulator sections (scrambled), hard x-ray self-seeding (HXRSS) chicane and the variable post-crystal undulator sections. The resulting x-rays are intercepted by a double crystal monochromator at XPP and output spectrum is measured with a spectrometer in the X-ray transport tunnel (XRT).

The final mean spectrum was then obtained by first subtracting the smoothed background set from the 0x0 configuration (no optimized undulators) and then taking the mean across all shots for a given seeding configuration. Using the filtered dataset and averaged signal from the detector, we then examined the spectra produced with seven initial HXUs and varying numbers of post-crystal undulators.

As the number of downstream undulators was reduced, the strength of the seeded signal decreased accordingly as shown in shown in Fig. 2. For the 7+9 case, the self-seeded peak is prominent while it gradually diminishes for 7+8 and so on. Most importantly, the spectrum for the 7+7 configuration still displays a clearly visible self-seeded signal, which is a key result of this study. For the 7+6 case, the seeded peak becomes marginal, and by 7+5 the self-seeded signal is no longer distinguishable from the SASE pedestal background.

In addition to the (220) reflection at 40.14° for 7.625 keV, the (400) reflection was also tested for self-seeding. At this energy, the (400) Bragg angle is 65.75°, which is closer to backscattering and results in a narrower energy acceptance. The acceptance bandwidth can be calculated following the relation,

$$\Delta E = \frac{\Delta\theta * E_0}{\tan(\theta_B)}\,, \tag{1}$$

where $\Delta\theta$ is the Darwin width of the reflection, E_0 = 7.625 keV is the experimental photon energy, and θ_B is the Bragg angle. For the (400) reflection at 7.625 keV, $\Delta\theta$ = 16.85 μrad and θ_B = 65.75°, which leads to an energy acceptance of ΔE = 58 meV. In comparison, for the CBXFEL design photon energy of 9.831 keV, the (400) Bragg angle of θ_B = 45° and the Darwin width is $\Delta\theta$ = 7.56 μ results in a broader energy acceptance ΔE = 74 meV. This implies that in the 7+7 configuration at 7.625 keV, the observation of a visible and measurable self-seeding peak in the spectrum using the (400) reflection with its narrow ΔE = 58 meV bandwidth is particularly relevant. Since at 9.831 keV, the (400) reflection would offer a larger acceptance bandwidth at ΔE = 74 meV and support the feasibility of achieving the two-pass gain with higher confidence.

The recorded 7+7 spectrum is further highlighted in Fig. 3 where three distinct features can be observed: the broad

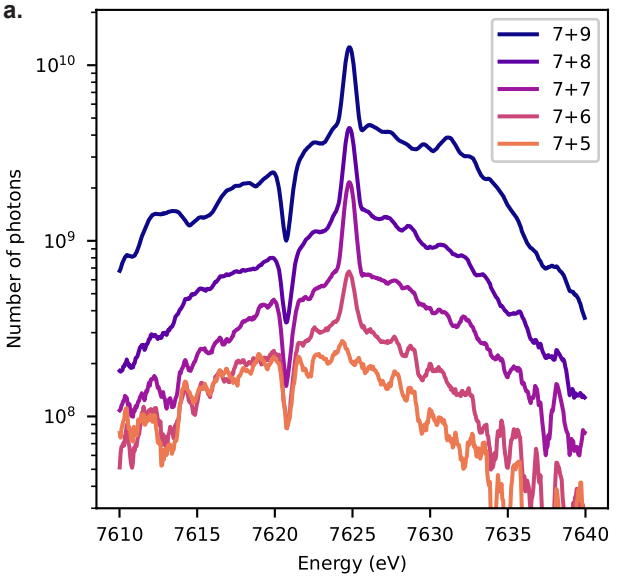

Figure 2: **a.** Comparison of measured X-ray spectrum intensity as a function of post-crystal undulators in logarithmic scale. **b.** Average '7 plus 7' measured spectrum displaying distinct features such as self-seeding peak, monochromator notch, and SASE distribution.

hump associated with self-amplified spontaneous emission (SASE) pedestal, a sharp dip (notch) due to diffraction in the XPP monochromator downstream, and the sharp peak indicating the self-seeded signal. To quantify the strength of the self-seeded peak, we calculated the gain ratio by taking the difference between the self-seeded peak a and the SASE top b and normalizing it to the top of a baseline 7×0 case c (no post-crystal undulators). This ratio $G = (a - b)/c$ provides a metric of seeding amplification and was applied across both the (220) and (400) crystal datasets using the same 7×0 baseline for comparison. For benchmarking purposes simulations were performed using GENESIS, in which the 7+7 configuration was simulated by taking the output field of 7 HXUs and feeding it as input for self-seeding crystal. The numerical simulations with a start-to-end beam corroborate the results displayed in Fig. 3.

ISBN: 978-3-95450-261-5 ISSN: 2673-7000 doi: 10.18429/JACoW-NAPAC2025-THP030

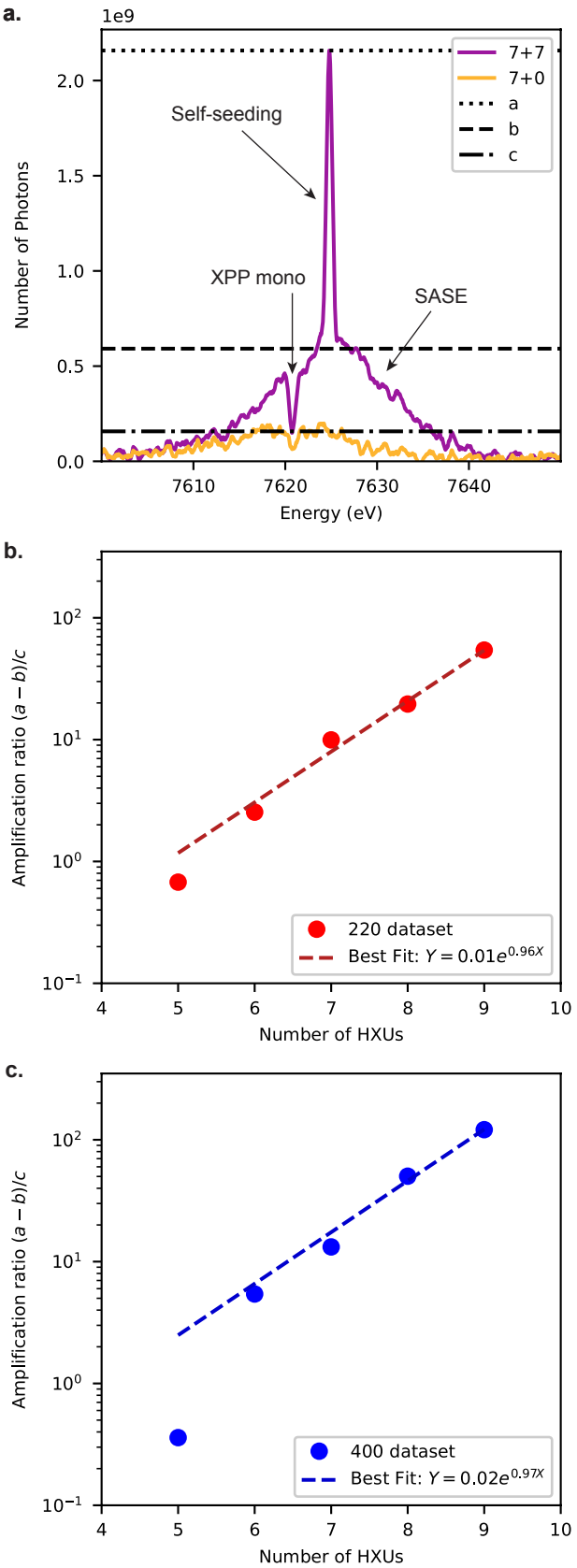

Figure 3: Amplification ratio as a function of post-crystal HXUs. **a.** 220 crystal dataset and **b.** 400 crystal dataset.

DISCUSSION

While the 7+7 self-seeding configuration demonstrated successful lasing in a single-bunch mode, replicating this performance in the full two-bunch CBXFEL mode presents significantly greater challenges. In practice, optimal lasing occurs when slices of the electron bunch with ideal phase-space characteristics are spatially on axis and temporally matched with the seed pulse. If both bunches are independently optimized, this overlap condition should be satisfied. However, in two-bunch operation, it is likely that when one bunch is optimized for lasing, the other is not fully optimized. This implies a fundamental trade-off between optimizing the first bunch for seed generation and the second for gain [9].

This trade-off becomes more manageable as more independent control knobs are introduced into the system. For example, the implementation of fast kickers upstream allow for control of the beam centroid angle and position. Energy control could be achieved through adjustments in the PSK and tuning of RF timing. Compression can be adjusted through the laser arrival time in the gun, although it remains difficult to achieve precise control over independent bunches.

Another key difficulty lies in achieving precise temporal and spatial overlap between the recirculating X-ray seed pulse and the second, fresh electron bunch. This overlap is a challenging requirement, it must occur at the entrance of the undulator beamline to ensure the most effective high-gain operation.

All these factors highlight the importance of further developing machine configuration strategies and diagnostic tools to support two-bunch lasing in CBXFEL. As accelerator tuning techniques evolve to provide more specific control over bunch-by-bunch properties, the feasibility of achieving two-pass gain CBXFEL operation will improve.

CONCLUSION

The 7+7 self-seeding measurements serve as a valuable test case for emulating the two-pass gain mechanism proposed in the CBXFEL project. By using the output of seven initial undulators to seed a second set of seven via a self-seeding crystal, this experiment demonstrates that effective seeding and FEL gain are achievable with just seven undulators. The clear observation of a seeded signal using both (220) and (400) diamond crystal reflections at 7.625 keV validates the feasibility of this approach. These results provide a strong foundation for the upcoming CBXFEL two-bunch demonstration, suggesting that seeding with seven undulators is sufficient to initiate amplification in a second pass. Moving forward, further refinement of accelerator tuning strategies for two-bunch operation will be essential.

ACKNOWLEDGEMENTS

This work is supported by U.S. Department of Energy Contract No. DE-AC02-76SF00515. We thank N. Burdet, T. Maxwell (SLAC) and the team of LCLS operators.

ISBN: 978-3-95450-261-5 ISSN: 2673-7000 doi: 10.18429/JACoW-NAPAC2025-THP030

REFERENCES

[1] J. Amann *et al.*, "Demonstration of self-seeding in a hard X-ray free-electron laser", *Nature Photonics*, vol. 6, no. 10, p. 693-698, Oct. 2012. doi:10.1038/NPHOTON.2012.180

[2] R. Margraf *et al.*, "Low-loss stable storage of 1.2 Å X-ray pulses in a 14 m Bragg cavity", *Nature Photonics*, vol. 17, no. 10, p. 878-882, Oct. 2023. doi:10.1038/s41566-023-01267-0

[3] K. J. Kim, Y. Shvyd'ko, and S. Reiche, "A proposal for an X-ray free-electron laser oscillator with an energy-recovery Linac", *Physical Review Letters*, vol. 100, no. 24, p. 244802, Jun. 2008. doi:10.1103/PhysRevLett.100.244802

[4] W. Qin *et al.*, "Start-to-end simulations for an X-ray FEL oscillator at the LCLS-II and LCLS-II HE", in *Proc. FEL'17*, Santa Fe, NM, USA, Aug. 2017, pp. 247–250. doi:10.18429/JACoW-FEL2017-TUC05

[5] Z. Huang and R. D. Ruth, "Fully coherent X-ray pulses from a regenerative-amplifier free-electron laser", *Physical Review Letters*, vol. 96, no. 14, p. 144801, Apr. 2006. doi:10.1103/PhysRevLett.96.144801

[6] G. Marcus *et al.*, "Regenerative amplification for a hard X-ray free-electron laser", in *Proc. FEL'19*, Hamburg, Germany, Aug. 2019, pp. 118–121. doi:10.18429/JACoW-FEL2019-TUP032

[7] M. D. Balcazar *et al.*, "Early lasing at LCLS and its implications for future cavity-based XFELs", in *Proc. IPAC'24*, pp. 424–427. doi:10.18429/JACoW-IPAC2024-TUPF12

[8] K. J. Kim, Z. Huang, and R. Lindberg, "Practical considerations and experimental results for high gain FELs", in Synchrotron Radiation and Free-Electron Lasers, Combridge, UK: Cambridge University Press, Mar. 2017. doi:10.1017/9781316677377

[9] C. Pellegrini, A. Marinelli, and S. Reiche, "The physics of X-ray free-electron lasers", *Reviews of Modern Physics*, vol. 88, no. 1, p. 015006, Mar. 2016. doi:10.1103/RevModPhys.88.015006